Rheol Acta (2006) 45: 943–950
DOI 10.1007/s00397-006-0086-2

ORIGINAL CONTRIBUTION

Erik Miller
Sung Jin Lee
Jonathan P. Rothstein

The effect of temperature gradients on the sharkskin surface instability in polymer extrusion through a slit die

Received: 22 August 2005
Accepted: 18 January 2006
Published online: 25 April 2006

E. Miller · S. J. Lee ·
J. P. Rothstein (✉)
Department of Mechanical Engineering,
University of Massachusetts,
Amherst, MA 01003-2210, USA
e-mail: rothstein@ecs.umass.edu

Abstract The sharkskin surface instability is commonly observed in the extrusion of polymer melts. We present a series of experiments in which a specifically designed rectangular slit die with insulated and independently heated sides and is used to induce precise temperature gradients across a flowing polyethylene melt. Our previous experiments demonstrated that the character of the surface distortions produced by the sharkskin instability was a function of the die wall temperature and therefore the extrudate had viscoelastic properties at the surface. In this paper, we explore the role of temperature and viscoelastic property gradients near the capillary wall. The amplitude of the sharkskin instability is quantified and plotted against apparent shear and extension rates. Analysis of the data demonstrates that the amplitude and frequency of the instability is independent of bulk temperature and temperature gradient and is dependent only on wall temperature. The data are normalized using a dimensionless Weissenberg number based on the extension rate to collapse the data collected over all temperatures and gradients onto a single master curve. We conclude with an example of a rectangular extrudate exhibiting varying surface roughness due to differential die heating and discuss the implications of our observations on the sharkskin surface instability mechanism and on commercial applications.

Keywords Polyethylene extrusion · Slit geometry · Sharkskin · Surface instability · Temperature gradients

Introduction

Commercial polymer processing methods, including blow molding and extrusion, are very sensitive to flow instabilities that develop when molten polymers are forced through an orifice die. The phenomenon, which has come to be known as sharkskin, is a surface instability characterized by a transition, at a critical stress, from smooth to a nearly periodic ridge-like surface distortion. Flow instabilities in extrusion were first observed after World War II, and the earliest reports of sharkskin were made by Howells and Benbow (1962) and Tordella (1963). Over the last 50 years, a great deal of research has focused on the characterization, elimination, and control of these flow instabilities. Several excellent reviews exist on flow instabilities, including those by Petrie and Denn (1976) and by Larson (1992). A more specific review with a focus on sharkskin can be found in Denn (2001).

Suppression of the sharkskin surface instability in the polymer extrusion process has motivated a great deal of research due to its limiting effect on commercial output rates. The underlying physical cause of this elastic instability is still widely debated in the literature and will be discussed in detail in the sections that follow. There is, however, a consensus in the literature that the instability is a result of the stress singularity developed at the die exit (Arda and Mackley 2005). A schematic diagram of the flow is shown in Fig. 1. The fluid along the surface of the

die is accelerated from a velocity of zero to that of the plug flow as it exits the capillary producing enormous stresses at the die exit.

Ramamurthy (1986) proposed a physical model which attributes sharkskin to a failure of adhesion at the polymer/die interface. Kalika and Denn (1987) supported this mechanism and described it in terms of a periodic slip at the die exit followed by nearly complete slip in the gross melt fracture regime. Later work by El Kissi and Piau (1994) contradicted this mechanism, however, suggesting that the slip at the wall reported by the previous studies was due to shear thinning. They concluded that sharkskin in linear low-density polyethylene (LLDPE) is caused by a cracking of the fluid at the die exit, where local stresses exceed the melt strength. Piau et al. (1989) noted that this surface melt fracture is cyclic in nature and is an exit phenomenon related to the relaxation of stretch strains. As opposed to cracking, Inn et al. (1998) describe the mechanism as a sticking and subsequent peeling of the polymer melt from the rim of the die. Numerical simulation results by Mackley et al. (1998) referred to the mechanism as a periodic melt rupture at the die exit resulting from the large velocity gradients, deformations, and stresses confined to the surface region. Despite the minor contradictions, the mechanism of sharkskin is fundamentally rooted in the kinematics of the flow near the die exit and the tensile stresses resulting from the stress singularity.

A variety of approaches to the issue of control have been explored. Researchers have employed several distinct methods to eliminate sharkskin. Most of these approaches, however, fall into two major categories: the addition of slip-promoting additives and modification of the die surface and materials. Inn et al. (1998) demonstrated that suppression of the instability was possible using a simple soap solution applied to the exterior of the die. Dhori et al. (1997) had success in coating the die in flouroelastomers and Migler et al. (2001a) demonstrated almost complete suppression by mixing fluoropolymer processing additives with LLDPE resin. Piau et al. (1995) used Teflon inserts to eliminate sharkskin. Ramamurthy (1986), Ghanta et al. (1998), and Perez-Gonzalez and Denn (2001) showed the successful suppression of the instability using alpha-brass dies. Another approach, pioneered in some of the earliest work by Cogswell (1977), suggested that varying die temperature can forestall the instability. This method addresses sharkskin on the basis of affecting the properties of the polymer itself, with the goal of reducing polymeric stress and deformation at the die exit. The theory of time–temperature superposition couples changes in viscosity and relaxation time to changes in temperature (Bird et al. 1987). Polymers are very sensitive to changes in temperature, such that raising the temperature decreases the viscosity exponentially. It is well known in industry that reducing the fluid viscosity and elasticity reduces surface distortions (Chung 2000, Michaeli 1984). Specific and localized die heating, however, is an approach that was later quantified by Miller and Rothstein (2004).

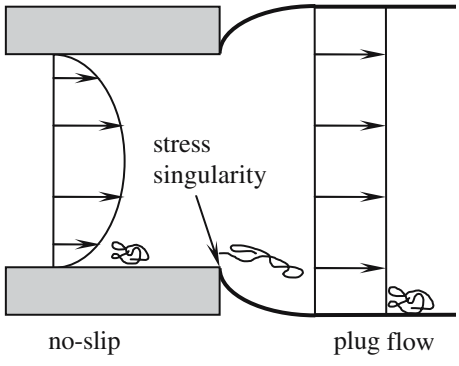

Fig. 1 Schematic diagram of a capillary die exit geometry showing no-slip wall condition and plug flow in the extrudate, with inherent stress singularity. High local stresses at the die exit plane result in strong deformation of the polymer chains and large tensile stresses

We previously showed that the onset condition and amplitude of sharkskin was dependent only on the temperature and the properties of the fluid adjacent to the die wall. In this paper, we present a series of experiments investigating the role of temperature gradients across the die on the surface instability. Rutgers et al. (2002) have already demonstrated qualitative results, in which temperature gradients between the inner and outer die lips in a film blowing application, produce smooth and sharkskin surfaces on the respective surfaces of a bubble. In our previous experiments, a capillary die was used with heating confined to the very end of the die. The goal was to generate a very thin thermal boundary layer and demonstrate that with very little addition of energy, the sharkskin could be eliminated or controlled by modifying the temperature and therefore, the rheological properties very near to the exit lip. However, with our previous design, it was difficult to precisely control the temperature gradients near the wall. Because the thermal boundary layer was not fully developed, the strength of the radial temperature gradients was affected by the flow rate. At very low flow rates, the Peclet number was extremely small resulting in a nearly constant temperature profile across the die. As the flow rate was increased, the thickness of the thermal boundary layer decreased. In the experiments detailed in this paper, a specifically designed rectangular die was used. The design is such that opposite sides of the die are insulated from each other and the temperature of each face is controlled independently. Using this die, we will induce a uniform and fully developed temperature profile across the flow allowing us to systematically study the importance of temperature gradients and rheological gradients on the sharkskin instability.

In the following section of this paper, we briefly discuss our experimental setup, working fluid, and test protocol. In the next section, we present our results demonstrating the effect of temperature gradients on the sharkskin surface instability. Finally, we conclude with some implications on

the mechanism of the elastic instability and make suggestions on the use of our technique for industrial extrusion.

Experimental

Apparatus

The experiments were performed on a previously built extruder which is described in detail in our previous work (Miller and Rothstein 2004). The extruder consists of a barrel with an internal volume of 0.19 m^3 and a stainless steel die. The system is heated by a combination of large band and small cylindrical cartridge heaters, for the barrel and die, respectively. Temperature is monitored by internal bore thermocouples in the barrel and surface mount thermocouples on the die and controlled with a series of standard PID controllers. A rectangular die was designed and fabricated for these experiments. In Fig. 2, a schematic diagram highlights the details of the die. A Teflon sheet was used as a thermal break between the upper and lower components of the die. By heating each wall of the die with an individually controlled cartridge heater, designated zones 1 and 2, a sustainable temperature gradient of greater than 20°C between the inner walls of the rectangular channel was achievable. The channel itself had a width of W=10 mm, a height of H=2 mm, and a length of 50 mm. It should be noted that although the ratio of width to height is relatively low (W/H=5), end effects typically caused in small channels are minimized due to the Teflon side walls, which have been shown to forestall the development of sharkskin. Additionally, the sharkskin will be characterized near the centerline of the extrudate to minimize the influence of the end effects.

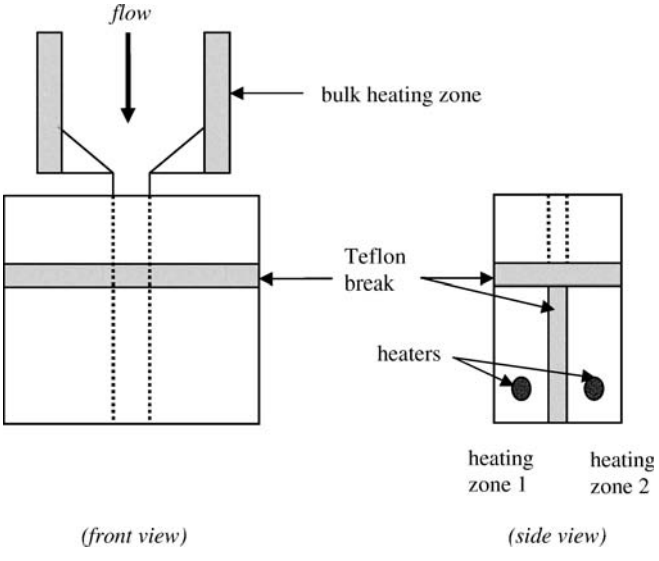

Fig. 2 Schematic diagram of experimental extruder with rectangular die

Working material

The polymer used in these experiments is a polyolefin plastomer, specifically, a copolymer of ethylene and octene. Dow AFFINITY EG8100 is a well-stabilized and commercially available LLDPE, as described in Migler et al. (2001a). EG8100 was delivered in pellet form and in the absence of any instability is almost completely transparent. Dynamic and steady flow rheology experiments were performed using parallel plate geometry on an AR2000 shear rheometer (TA Instruments). For completeness, the rheology of the fluid is characterized by a viscosity weighted-average relaxation time of $\overline{\lambda} = 1.52\text{s}$ and a zero-shear rate viscosity of $\eta_0 = 4.0 \times 10^4\ \text{Pa} \cdot \text{s}$ at a working temperature of T=140°C. Shifting of the linear viscoelastic data over a range of temperatures using the Arrhenius form of the time–temperature superposition shift gave an activation energy of $\Delta H/R$=3,460 K, which was used in later calculations. A full characterization on the same batch of polymer can be found in Miller and Rothstein (2004).

Experimental protocol

The rectangular die design was calibrated by generating flow curves correlating the measured pressure drop supplied to the extruder against the mass output rate of the polymer extrudate from the die. Timed samples were collected and weighed to calculate the mass flow rate. This procedure was done for several different temperature conditions, both with and without die temperature gradients. To examine the effects of temperature gradients between walls of the slit die, it was necessary to select an acceptable range of working temperatures. A temperature range of 100 to 120°C was selected in order to maximize the amount of data that could be collected before the supply of molten polymer was exhausted from the extruder barrel.

Unlike previous experiments with capillary dies producing cylindrical extrudates (Miller and Rothstein 2004), the rectangular samples had two surfaces of interest. Samples were collected, allowed to cool, and then carefully cut into slices following the direction of extrusion. The slices were then marked according to which heating zone produced the surface. In the cases with the highest heating difference between heating zones 1 and 2, the extrudate samples were observed to curl towards the lower temperature side. This curling is a result of the viscosity difference across the extrudate resulting from the imposed temperature gradient. The viscosity gradient results in an antisymmetric velocity profile across the channel and a curling of the extrudate towards the slower moving and more viscous side. The

samples were allowed to develop until they had enough mass to fall down and draw the emerging extrudate straight out with little deflection. The curled end was discarded and samples were taken from straighter sections where there was little distortion to the sharkskin surface. Careful record keeping was necessary for this data collection, as each slice was produced by a unique combination of flow rate, bulk heating, and differential die heating. The slices were photographed under a microscope, providing up to two data points per slice for the case of die temperature gradients. Sharkskin amplitude and wavelength data were acquired from the photographs using the same process and digital analysis routine designed for our previous sharkskin experiments (Miller and Rothstein 2004).

Experimental results and discussion

A characteristic photo of a sharkskin surface is shown in Fig. 3. The parameter of most interest, both in previous and current experiments, is the amplitude, A, of the nearly periodic sharkskin surface instability. The first set of results describing the amplitude behavior for this system is shown in Fig. 4. In this figure, amplitude is plotted against an average or apparent shear rate calculated assuming infinite parallel plates, $\dot{\gamma}_{app} = 6\overline{V}/H$, where H is the height of the slit and the average velocity, $\overline{V} = \dot{m}/\rho HL$, is calculated from the measured mass flow rate, $\dot{m}$, and the cross-sectional area of the slit die. Experiments were conducted at a constant temperature in the die and bulk to provide a baseline upon which to compare data resulting from temperature gradients between the die walls. As expected, within each data set shown in Fig. 4, the results display an increase in the sharkskin amplitude with increasing shear rate and decreasing temperature.

The addition of a temperature gradient between the walls of the die produces some interesting results. A composite image illustrating the profile of a rectangular extrudate

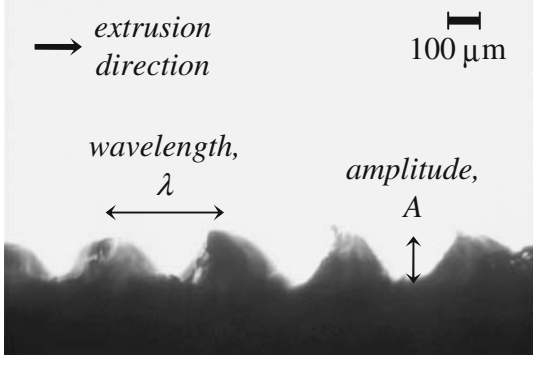

Fig. 3 Characteristic profile photo of EG8100 extrudate with fully developed sharkskin surface

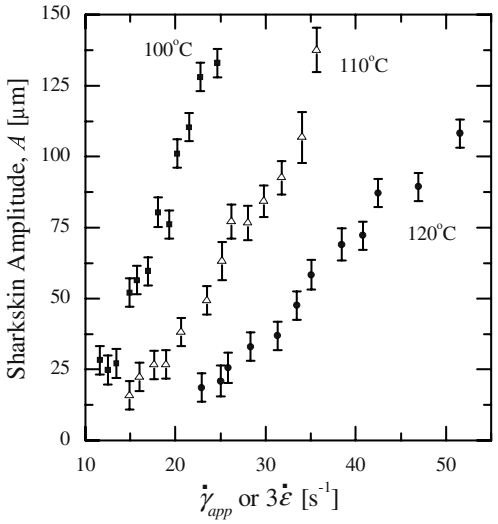

Fig. 4 Sharkskin amplitude as a function of average shear rate or equivalent extension rate at constant temperature conditions in bulk and die heating zones, $T_{bulk}=T_1=T_2$. Three sets of data shown at T=100, 110, and 120°C

produced by a slit with temperature gradients is shown in Fig. 5. This is a composite image created by using two photographs of opposite sides of the same extrudate sample. This image clearly demonstrates that the localized die temperature and the temperature of the fluid close to the die wall are the primary factors contributing to the character of the extrudate surface (Miller and Rothstein 2004). What remains to be seen are what effects temperature gradients across the extrudate will have. The geometry of the slit die made it possible to impose linear temperature gradients, up to 10°C/mm, across the flow. By employing a long slit die, both the velocity and temperature profile within the flow were given the necessary residence time to become fully developed. In the flow through a channel, the hydrodynamic and thermal entrance lengths can be estimated from (Mills 1999):

$$\frac{L_{hydrodynamic}}{D_h} \simeq 0.05\, Re_D, \tag{1}$$

$$\frac{L_{thermal}}{D_h} \simeq 0.033 Re_D\, Pr\,, \tag{2}$$

where the hydraulic diameter, $D_h=4A/P\simeq 2H$, for cross-sectional area, A, and perimeter, P, is approximately twice the spacing of the plates in the limit of a large aspect ratio rectangular channel. In our experiments, D_h=4 mm. For our experiments, the Reynolds number was less than $Re_D = \rho\overline{V}D_h/\eta \leq 9\times 10^{-7}$ and the Prandtl number was $Pr = \eta/\rho\alpha = 2\times 10^{8}$. The large Prandtl number is due

to a combination of the large viscosity and the low thermal conductivity of the polyethylene, $(\alpha = 2 \times 10^{-7})$, and dictates that the thermal entrance length calculated from Eq. 2 will be much longer than that of the hydrodynamic entrance length. For our extrusion experiments, the maximum hydrodynamic and thermal entrance lengths calculated from the Reynolds and Prandtl numbers above are calculated from Eqs. 1 and 2 as $L_{hydrodynamic} = 2 \times 10^{-7}$mm and $L_{thermal}$=24 mm, respectively. These calculations indicate that with the channel length of 50 mm, both the temperature and the velocity profiles become fully developed well in advance of the die exit for all of the experiments presented here.

A series of experiments was performed in which the difference between the die temperatures in both heating zones and the bulk temperature were varied to produce a temperature gradient varying from 0 to 10°C/mm. The results are shown in Fig. 6. It was noted earlier that experiments in which there was a die temperature gradient produced a slightly curled extrudate as a result of a variance in the viscosity of the fluid at the walls. For this reason, it is important to note that the shear rates we will use are average or apparent shear rates based on the measured volume flow rate. The result is that for experiments involving temperature gradients across the capillary, the apparent shear rate will underestimate the true shear rate at the hot wall and overestimate at the cold wall. We will discuss this important point in more detail in the following paragraphs.

As alluded to by the image shown in Fig. 5, each extrudate sample contains two sets of data, one for each surface. The wall temperatures in zones 1 and 2 were varied from 100 to 110 and 120°C to produce temperature gradients of 0, 10, and 20°C across the gap. Overlaid on the results from Fig. 4, the data in Fig. 6 exhibit the same patterns of increasing sharkskin amplitude with increasing shear rate and decreasing amplitude for corresponding shear or extension rates with decreasing wall temperature. More notably, the results in Fig. 6 show that the amplitude of the sharkskin surface appears to be independent of the temperature gradient. For both cases of ΔT=10°C, and the single case of ΔT=20°C, the amplitude data falls on top of the corresponding temperature for the cases of constant temperature. In other words, three distinct trends corresponding to T_{wall}=100, 110, and 120°C can be seen in Fig. 6, independent of temperature gradients. Furthermore, bulk temperature of the fluid entering the die was varied from matching one of the wall conditions to splitting the difference between the two in order to promote a more uniform temperature gradient. The bulk temperature was found to have no apparent effect on the amplitude results confirming that the temperature profile was indeed fully developed as suggested by Eq. 2. These quantitative results indicate that even with developed and sustained temperature gradients across the extrudate, the sharkskin surface instability is related only to the properties of the fluid directly adjacent to the die wall and independent of any internal gradients.

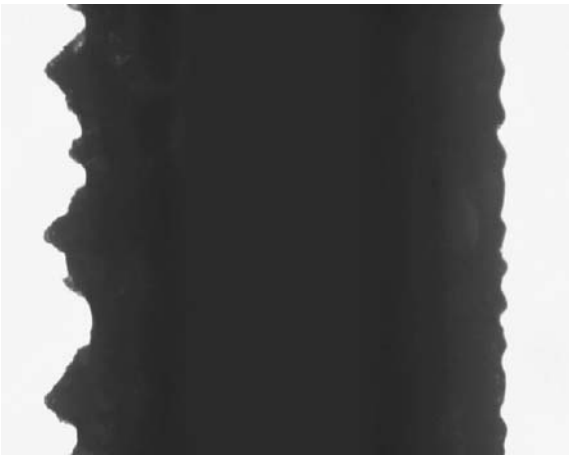

Fig. 5 Composite of two edge profile images from either side of the same rectangular extrudate sample showing distinct surface roughness as a result of die temperature gradient. The left side was at $T_{wall,\ 1}$=100°C, while the right side was at $T_{wall,\ 2}$=120°C, with a bulk temperature, T_{bulk}=110°C

The time–temperature superposition shift factor tells us that viscosity and relaxation time scale proportionally with changes in temperature (Bird et al. 1987):

$$a_T = \frac{\lambda(T)T}{\lambda(T_{ref})T_{ref}} = \frac{\eta(T)}{\eta(T_{ref})}. \tag{3}$$

The Weissenberg number describes the ratio of the characteristic fluid relaxation time to the extension rate or shear rate, and is typically used with steady flow, as defined by Morrison (2001). If one ignores the shear rate dependence of the viscosity for the moment, then it can be shown that the local Weissenberg number evaluated with the shear rate and temperature at each wall of the die can be written as:

$$\begin{aligned} Wi_w &= \dot{\gamma}_w \lambda(T_w) = \frac{\tau_w}{\eta(T_w)} \lambda(T_w) \\ &= \frac{\tau_w}{\eta(T_{ref})} \lambda(T_{ref}) \frac{T_{ref}}{T_w}. \end{aligned} \tag{4}$$

Here, τ_w is the shear stress at the wall. Thus, for a constant-viscosity fluid in this rectangular die, the Weissenberg number based on the shear rate is roughly constant across the gap and nearly independent of the local wall temperature or temperature gradient. This analysis suggests that for a constant-viscosity fluid, the kinematics within the die are unaffected by the temperature gradient across the die and should have little effect on the polymer deformation or stretch near the walls. For this special case, it is unlikely

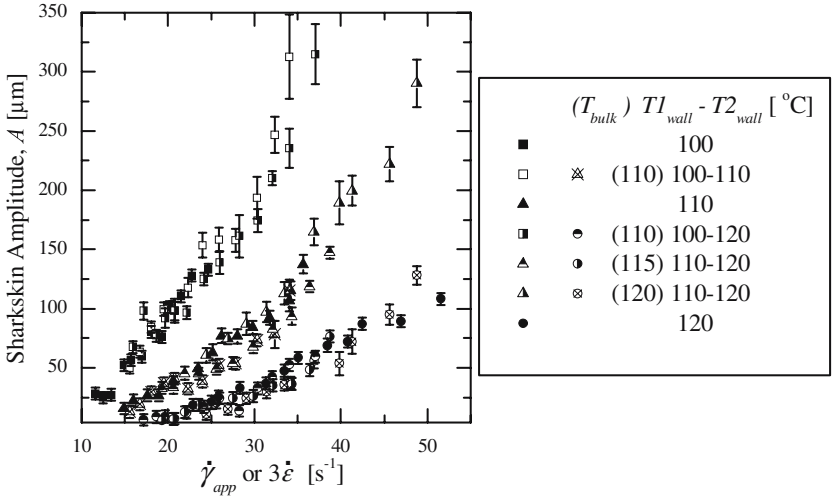

Fig. 6 Sharkskin amplitude as a function of average apparent shear rate or equivalent extension rate at various die temperature gradient conditions. Constant temperature conditions shown in *filled symbols*, gradient conditions (two points per sample) shown in *open symbols*, shape to match set wall temperature

that the shear flow within the die dictates the stability of the extrudate. If we now assume a power law profile in the viscosity and relaxation time such that $\eta = \alpha_n \dot{\gamma}^{n-1}$ and $\lambda = \beta_m \dot{\gamma}^{m-1}$, where n=0.8 and m≅0.3 (Miller and Rothstein 2004), then the Weissenberg number becomes:

$$Wi_w = \left(\frac{\tau_w}{\alpha_n(T_{ref})}\right)^{\frac{m}{n}} \beta_m(T_{ref}) \left(\frac{T_{ref}}{T_w}\right) a_T^{\left(\frac{n-m}{n}\right)}, \quad (5)$$

which is still a relatively weak function of temperature. Using this definition of the Weissenberg number, the data in Fig. 6 will not collapse into a single master curve. In fact, the variance of the amplitude data increases as the difference in local shear rate between the hot and cold wall increases with increasing temperature gradient. If, however, we examine the extensional flow at the exit of the die by forming a Weissenberg number defined with the extension rate,

$$Wi_{ext} = \lambda(T_w)\dot{\varepsilon} = \lambda(T_{ref})\dot{\varepsilon} a_T, \quad (6)$$

the correct temperature dependence is captured, and as seen in Fig. 7, the data from Fig. 6 collapse into a single master curve, the form of which will be discussed in more detail in the following sections.

The extension rate can be approximated as $\dot{\varepsilon} \cong 2\dot{Q}/H^2 L$, where we assume that the acceleration of the polymer from zero or nearly zero at or near the wall to the bulk mean velocity occurs over a length approximately equal to the half-width of the slit. It should be noted that velocity measurements within a circular die and extrudate performed by Migler et al. (2001b) showed that this acceleration can in fact occur over much shorter distances. However, even though our apparent extension rate may be small by a numerical constant, the determination of the exact value of the extension rate would require a priori knowledge or direct measurement of the flow field. Unlike the local shear rate within the die, our observations of the extrudate have shown that the extension rate is not a strong function of the fluid temperature. The Weissenberg number based on the extension rate, thus, becomes strongly temperature-dependent, varying linearly with the time–temperature superposition shift factor, a_T. Based on the preceding arguments and scaling, the data in Fig. 6 provide more insight when the amplitude of the elastic instability is viewed not as a function of shear rate, which is a strong function of the die wall temperature but as a function of extension rate which is nearly independent of the die wall temperature and is only a function of the flow rate and geometry. The extension rate

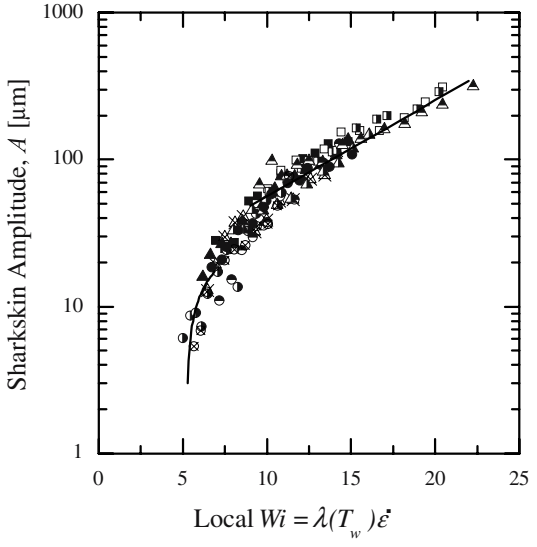

Fig. 7 Master curve of all amplitude data at temperature conditions from Fig. 6 using local Weissenberg number. Fits included for data near and far from onset of sharkskin instability; $A = 13.5(Wi - 5.3)^{1/2}$ and A=12.6$e^{0.15Wi}$, respectively

can then be written in terms of the previously defined apparent shear rate,

$$\dot{\varepsilon} \cong \dot{\gamma}_{\text{app}}/3, \tag{7}$$

and therefore,

$$Wi_{ext} \simeq Wi/3. \tag{8}$$

Using Eq. 6, we can convert the extension rate data from Fig. 6 into a nondimensional local Weissenberg number. For this calculation, the temperature-dependent relaxation time at the die wall, $\lambda(T_w)$, was evaluated using the Arrhenius form of the time–temperature superposition shift factor (Bird et al. 1987), where the shift factor was obtained from fitting of the dynamic rheology data. For a detailed description of these calculations, the reader is referred to our previous work (Miller and Rothstein 2004). By converting all of the extension rate data in Fig. 6 to a Weissenberg number, a master curve is formed and is shown in Fig. 7. The data, normalized based on their respective wall temperature conditions, collapse into a single trend. This collapse verifies that in the presence of temperature gradients, the character of the sharkskin surface is dictated by the temperature of the die wall and the strength of the extensional flow at the exit corners of the die. Additionally, it should be noted that the onset of the elastic instability in all cases occurs at Weissenberg numbers based on the extension rate which are much larger than, $Wi_{ext}>0.5$. At these Weissenberg numbers, the polymer chains will have undergone a coil-stretch transition resulting in significant hardening of the extensional viscosity and the development of large deformation and elastic stresses (Larson 1999).

Another feature of the data shown in Fig. 7 is that of a good fit to the asymptotic results for a supercritical Hopf bifurcation, the details of which are described by Iooss and Joseph (1980). In the region near the onset of the instability, the amplitude follows a power law behavior, $A = A_0(Wi_{ext} - Wi_{ext,crit})^{1/2}$, where $Wi_{ext,crit}$ is the critical Weissenberg number for the onset of the elastic surface instability and A_0 is a constant. The data in Fig. 7 fit this trend well, with parameters A_0=13.5 μm and $Wi_{ext,crit}$=5.3. When the local Weissenberg number is much larger than $Wi_{ext,crit}$, nonlinear dynamics begin to dominate the flow kinematics and the amplitude is found to grow exponentially with increasing Weissenberg number. When scaled using Eq. 8, the critical Weissenberg number based on extension rate for our experiments is in good agreement with values reported in the literature by Meulenbroek et al. (2003) and with the previous experiments of Miller and Rothstein (2004), where the critical Weissenberg number based on apparent shear rate was found to be Wi_{crit}=12. This lends further support to the observation that the sharkskin instability is a function of wall temperature and local extensional stress concentration at the die exit and is independent not only of temperature gradients, but also of die geometry and shear rate.

Our collective observations suggest that the underlying physical mechanism for the sharkskin surface instability is likely not a coil-stretch transition resulting from the shear flow within the die and involving polymer chains either tethered to or adjacent to the die wall as suggested by Barone et al. (1998) and Mhetar and Archer (1998). Whether the chains are tethered to the wall or not adsorbed, the coil-stretch transition is inherently dependant on the shear flow kinematics, the magnitude of the local shear rate, and interaction of the chains near the wall and other polymer chains in the shear flow that are entangled with them. Because the imposed temperature gradient affects the velocity and the shear rate profiles across the gap, one would expect that if the physical cause of the sharkskin instability were a shear-induced coil-stretch transition of polymer tethered to or near the die wall, then the local shear flow kinematics would have a significant effect on the frequency and/or amplitude of the instability. They do not. It, therefore, seems more likely that the underlying physical mechanism responsible for sharkskin stems from the enormous stresses generated in the strong extensional flow at the exit of the die, resulting in either an adhesive failure of the polymer along the die wall, as suggested by Migler et al. (2001b), a cracking or rupture of the extrudate surface at the die exit (Cogswell 1977; El Kissi and Piau 1994), or the sticking and subsequent peeling of the polymer melt from the rim of the die as suggested by Inn et al. (1998).

Conclusions

A series of molten polymer extrusion experiments have been performed using differential heating on opposite sides of a rectangular slit die to study the effects of large temperature gradients on the sharkskin surface instability. The temperature gradients were used to produce large gradients in the rheological properties of the molten polymer. By quantifying the amplitude and character of the distortions on the respective surface of the extrudate, the sharkskin instability was found to be independent of temperature gradients that were developed within the bulk molten polymer and was found to be dependent only on the temperature of the adjacent wall. Furthermore, the induced temperature gradient also caused a variation in the flow kinematics between each wall of the die with no apparent variation in the character of the instability when compared to uniform conditions. In our previous work (Miller and Rothstein 2004), we found that sharkskin amplitude is also essentially independent of upstream temperature and bulk properties and is therefore, easily controlled by minimal

and localized heating of the die exit corner. The resulting implications based on the mechanism of the sharkskin instability may have interesting application to commercial extrusion processes. With the proper design, our techniques could be implemented to manufacture specifically and variably textured extrudates.

Acknowledgement The authors would like to acknowledge the Executive Area for Research for partial support of this research through a Healy Endowment Grant.

References

Arda D, Mackley M (2005) The effect of die exit curvature, die surface roughness and fluoropolymer additive on sharkskin extrusion instabilities in polyethylene processing. J Non-Newton Fluid Mech 126:47–61

Barone JR, Plucktaveesak N, Wang SQ (1998) Interfacial molecular instability mechanism for sharkskin phenomenon in capillary extrusion of linear polyethylenes. J Rheol 42:813–832

Bird RB, Armstrong BC, Hassager O (1987) Dynamics of polymeric liquids: volume 1, fluid mechanics. Wiley, New York

Chung CI (2000) Extrusion of polymers: theory and practice. Carl Hanser Verlag, Munich

Cogswell FN (1977) Stretching flow instabilities at the exits of extrusion dies. J Non-Newton Fluid Mech 2:37–47

Denn MM (2001) Extrusion instabilities and wall slip. Annu Rev Fluid Mech 33:265–287

Dhori PK, Jeyaseelan RS, Giacomin AJ, Slattery JC (1997) Common line motion III: implication in polymer extrusion. J Non-Newton Fluid Mech 71:231–243

El Kissi N, Piau J-M (1994) Adhesion of linear low density polyethylene for flow regimes with sharkskin. J Rheol 38:1447–1463

Ghanta VG, Riise BL, Denn MM (1998) Disappearance of extrusion instabilities in brass capillary dies. J Rheol 43:435–442

Howells ER, Benbow JJ (1962) Flow defects in polymer melts. Trans J Plast Inst 30:240–253

Inn YW, Fisher RJ, Shaw MT (1998) Visual observation of development of sharkskin melt fracture in polybutadiene extrusion. Rheol Acta 37:573–582

Iooss G, Joseph D (1980) Elementary stability and bifurcation theory. Springer, Berlin Heidelberg New York

Kalika DS, Denn MM (1987) Wall slip and extrudate distortion in linear low-density polyethylene. J Rheol 31:815–834

Larson RG (1992) Instabilities in viscoelastic flows. Rheol Acta 31:213–263

Larson RG (1999) The structure and rheology of complex fluids. Oxford University Press, New York

Mackley M, Rutgers R, Gilbert D (1998) Surface instabilities during the extrusion of linear low density polyethylene. J Non-Newton Fluid Mech 76:281–297

Meulenbroek B, Storm C, Bertola V, Wagner C, Bonn D, Saarloos Wv (2003) Intrinsic route to melt fracture in polymer extrusion: a weakly nonlinear subcritical instability in viscoelastic Poiseuille flow. Phys Rev Lett 90:024502(4)

Mhetar V, Archer LA (1998) Slip in entangled polymer melts: 1. General features. Macromolecules 31: 8607–8616

Michaeli W (1984) Extrusion dies: design and engineering computations. Carl Hanser Verlag/Macmillan, Munich

Migler KB, Lavalee C, Dillon MP, Woods SS, Gettinger CL (2001a) Visualizing the elimination of sharkskin through fluoropolymer additives: coating and polymer–polymer slippage. J Rheol 45:565–581

Migler KB, Son Y, Qiao F, Flynn K (2001b) Extensional deformation, cohesive failure, and boundary conditions during sharkskin melt fracture. J Rheol 46:383–400

Miller E, Rothstein JP (2004) Control of the sharkskin instability in the extrusion of polymer melts using induced temperature gradients. Rheol Acta 44:160–173

Mills AF (1999) Heat transfer. Prentice Hall, Upper Saddle River, NJ

Morrison FA (2001) Understanding rheology. Oxford University Press, New York

Perez-Gonzalez J, Denn MM (2001) Flow enhancement in the continuous extrustion of linear low-density polyethylene. Ind Eng Chem Res 40:4309–4316

Petrie CJS, Denn MM (1976) Instabilities in polymer processing. AIChE J 22:209–236

Piau JM, El Kissi N, Tremblay B (1989) Influence of upstream instabilities and wall slip on melt fracture and sharkskin phenomena during silicones extrusion through orifice dies. J Non-Newton Fluid Mech 34:145–180

Piau J-M, Kissi NE, Toussant F, Mezghani A (1995) Distortion of polymer melt extrudates and their elimination using slippery surfaces. Rheol Acta 34:40–57

Ramamurthy AV (1986) Wall slip in viscous fluids and influence of materials of construction. J Rheol 30:337–357

Rutgers R, Clemeur N, Husny J (2002) The prediction of sharkskin instability observed during film blowing. Int Polym Process 17:214–222

Tordella JP (1963) Unstable flow of molten polymers: a second site of melt fracture. J Appl Polym Sci 7:215–229